Mineral Detection of Cosmic-Ray Boosted Dark Matter

Jin–Wei Wang

Physics Department, UESTC

Jin–Wei Wang, Fei–Fei Li; arxiv:2601.13949

Karlsruhe, April 15th, 2026

Outline

- Introduction and motivation
- CRDM flux calculation
- CRDM track length spectrum
- Paleo detector constraints
- Summary

Dark matter in the Universe

- The astrophysical and cosmological observations have provided compelling evidences of the existence of **dark matter (DM)**.

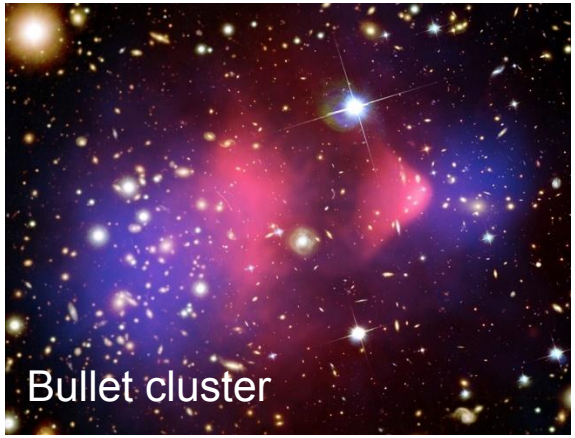

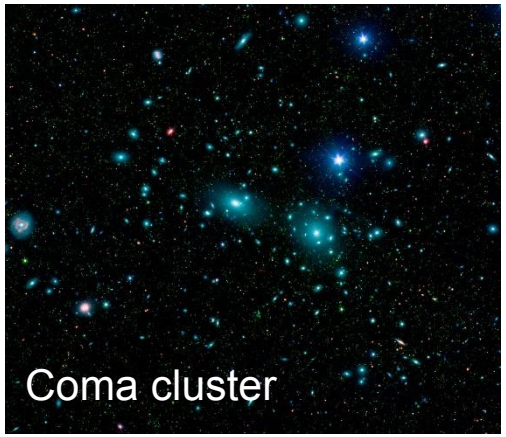

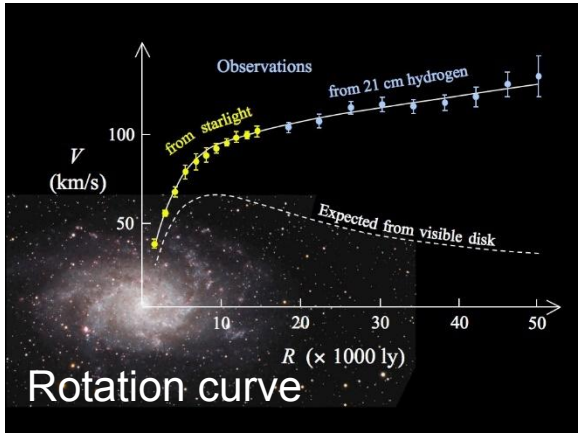

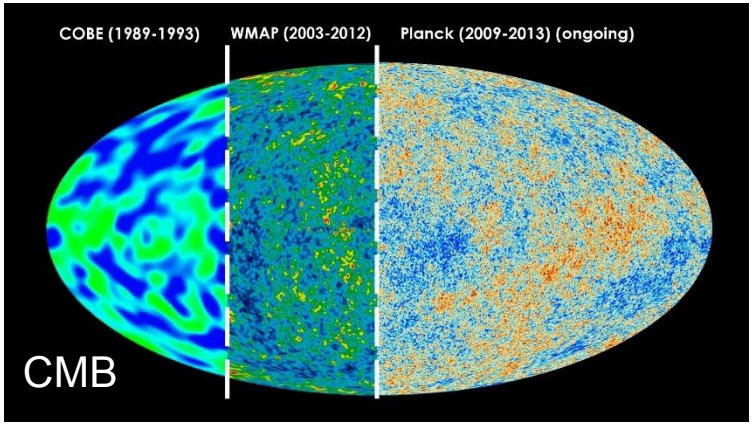

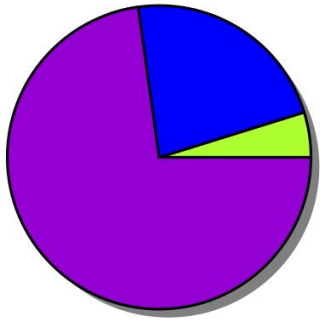

Planck 2018
[1807.06209]

Cold DM (~26%)

$\Omega_c h^2 = 0.11933 \pm 0.00091$

Baryons (~5%)

$\Omega_b h^2 = 0.02242 \pm 0.00014$

Dark energy (~69%)

$\Omega_\Lambda = 0.6889 \pm 0.0056$

DM direct detection

LZ Experiment, PRL (2025), 4.2 t·yr

Kinetic energy

$E_R \in [5.4, 55]$ keV

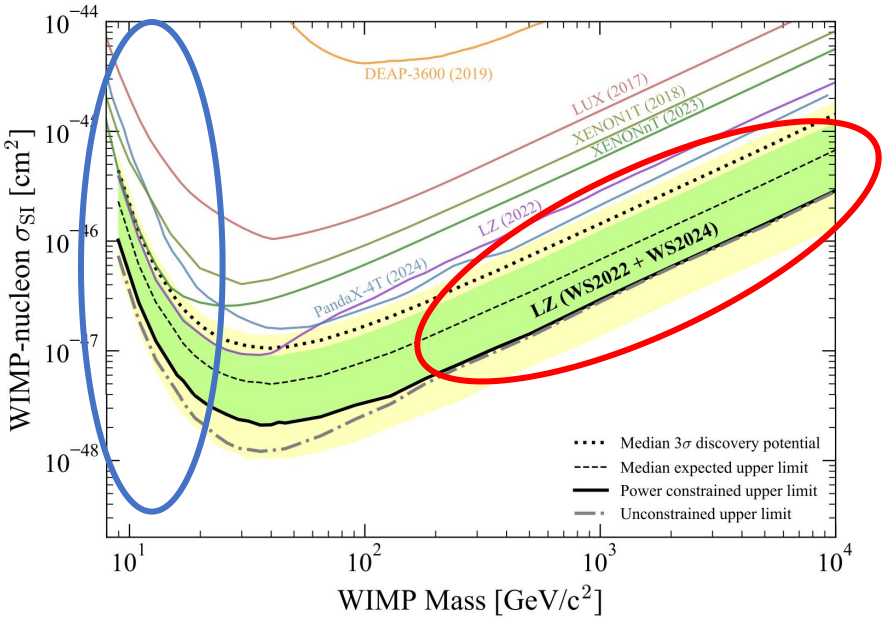

DM number density

$\sigma_{SI} \sim m_\chi$

- **Improve DM kinetic energy:** scattering between cosmic-ray particles and DM (CRDM); [1810.10543]
- **Reduce E_{th}:** Migdal effects; [1907.11485, 1707.07258]

Paleo detectors

- Ancient mineral provides a new way to serach for DM with large exposure

  ~$10^5\ t \bullet yr$

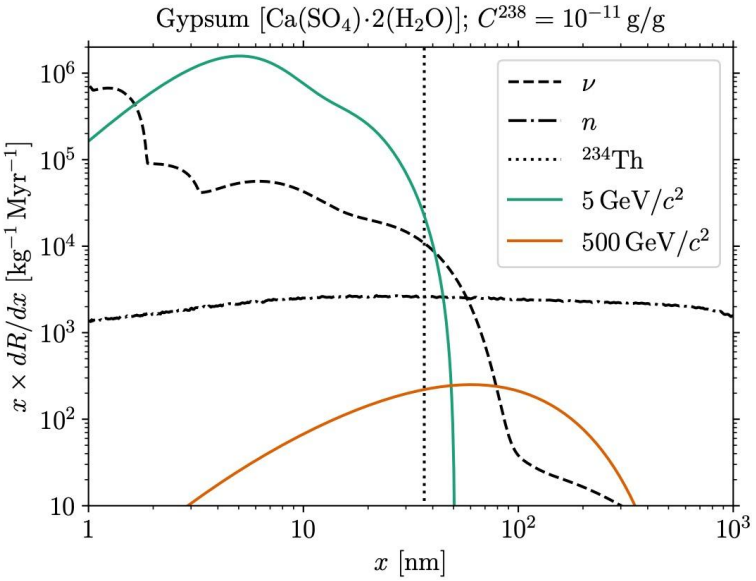

S. Baum et al. Instruments 2021

- CRDM may prodece longer tracks and supress the backgound!

CRDM + Paleo detectors

CRDM flux

- The local interstellar (LIS) population of CRs is well measured, and Galactic CR propagation and solar modulation are treated using GALPROP and HELMOD

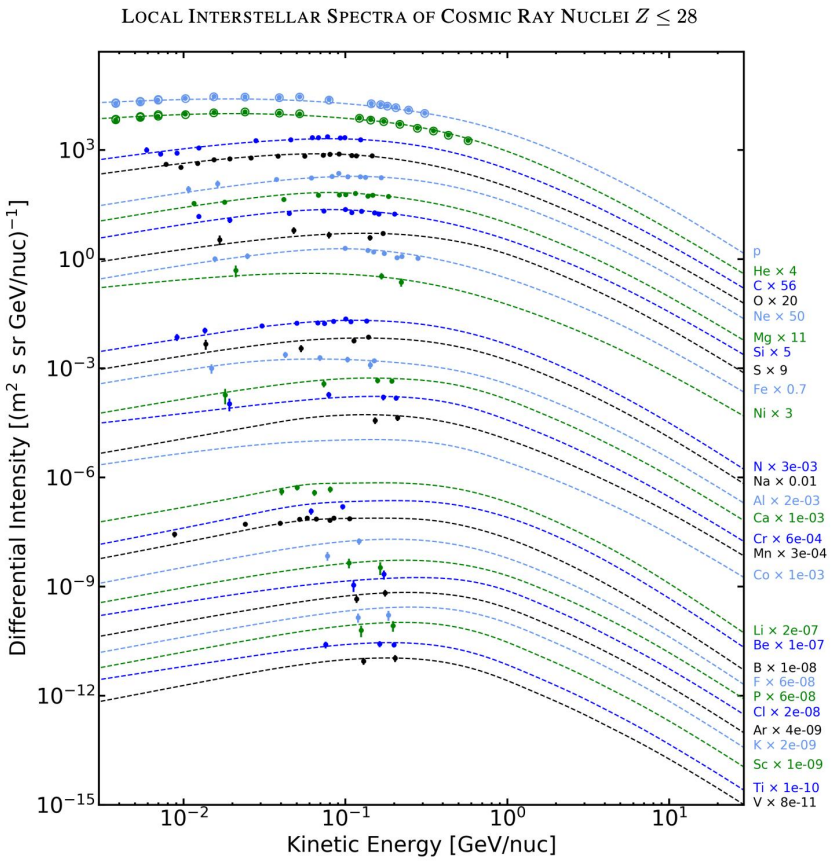

M. J. Boschini et al. ApJS 2020

CRDM flux

- The local interstellar (LIS) population of CRs is well measured, and Galactic CR propagation and solar modulation are treated using GALPROP and HELMOD
- We include the nine dominant CR species that account for more than 90% of the total CRDM flux, namely {H, He, C, N, O, Ne, Mg, Si, Fe}
- CRDM flux: $$\frac{d\Phi_\chi}{dT_\chi} = D_{\rm eff}\,\frac{\rho_\chi}{m_\chi}\sum_i \int_{T_i^{\rm min}(T_\chi)}^{\infty} dT_i\,\frac{d\sigma_{\chi i}}{dT_\chi}\,\frac{d\Phi_i}{dT_i}$$ with $\rho_\chi \simeq 0.3\ \mathrm{GeV\,cm^{-3}}$

The parameter D_{eff} represents the effective distance over which CR–DM scattering contributes to the local CRDM flux; throughout this work we take D_{eff} ≃ 9 kpc

C. Xia. et al. JCAP 2022

Model setup

Jin–Wei Wang, Fei–Fei Li; arxiv:2601.13949

- Consider two benchmark models:
  - constant DM–proton scattering cross section: $\sigma_{\chi p}$
  - $\mathcal{L} \supset \bar{\chi}(i\partial_\mu\gamma^\mu - m_\chi)\chi + g_\chi\bar{\chi}\gamma^\mu\chi V_\mu + \sum_q g_q\bar{q}\gamma^\mu q V_\mu + \frac{1}{2}m_V^2 V_\mu V^\mu$
- **Elastic scattering** between DM and nucleus
  - $\frac{d\sigma_{\chi i}}{dT_\chi} = A_i^2 \frac{G_i^2(Q^2)}{T_\chi^{\max}(T_i)} \frac{\mu_{\chi i}^2}{\mu_{\chi p}^2}\sigma_{\chi p}$ with $T_\chi^{\max}(T_i) = \frac{T_i^2 + 2m_i T_i}{T_i + (m_i + m_\chi)^2/(2m_\chi)}$
  - $\frac{d\sigma_{\chi i}^{\rm el}}{dT_\chi} = 2m_\chi \frac{A_i^2 g_p^2 g_\chi^2}{4\pi\beta^2} \frac{G_i^2(Q^2)}{(Q^2 + m_V^2)^2}\left[1 - \frac{\beta^2 Q^2}{Q_{\max}^2} + \frac{Q^4}{8m_\chi^2 E_i^2}\right]$ with $Q_{\max}^2 = \frac{4(E_i^2 - m_i^2)m_\chi^2}{m_\chi^2 + m_i^2 + 2m_\chi E_i}$.

For hydrogen and helium, we adopt the **dipole form factor**, while for heavier nuclei we use the **Helm form factor.**

Model setup

- **Deep inelastic scattering (DIS)** between DM and proton can be expressed with **Bjorken scaling variable x and y**

$$\frac{d^2\sigma_{\chi p}^{\rm DIS}}{dT_\chi d\mu_s} = \frac{m_\chi\sqrt{(T_p^2+2m_pT_p)(T_\chi^2+2m_\chi T_\chi)}}{m_p^2E_\chi^2 y}\frac{d^2\sigma_{\rm DIS}}{dxdy}$$

$$\frac{d^2\sigma_{\rm DIS}}{dxdy} = \frac{g_\chi^2 g_q^2}{4\pi(Q^2+m_V^2)^2}\frac{2E_\chi^2 y}{E_\chi^2-m_\chi^2}\left(1-y+\frac{y^2}{2}-\frac{xym_p}{2E_\chi}-\frac{m_\chi^2}{2E_\chi m_p}\frac{y}{x}\right)F_2(x,Q^2)$$

with the structure fucntioin $F_2(x,Q^2) = \sum_{f=u,d,c,s,b}\left[f(x,Q^2)+\bar{f}(x,Q^2)\right]x$

- For scattering on CR nuclei, we approximate

$$\frac{d^2\sigma_{\chi i}^{\rm DIS}}{dT_\chi d\mu_s} = R_i(x,Q^2)\left[Z_i\frac{d^2\sigma_{\chi p}^{\rm DIS}}{dT_\chi d\mu_s}+(A_i-Z_i)\frac{d^2\sigma_{\chi n}^{\rm DIS}}{dT_\chi d\mu_s}\right] \quad \text{with} \quad R_i(x,Q^2)\simeq 1$$

Integrating over the scattering angle ➡ $\frac{d\sigma_{\chi i}^{\rm DIS}}{dT_\chi} = \int d\mu_s \frac{d^2\sigma_{\chi i}^{\rm DIS}}{dT_\chi d\mu_s}$

CRDM spectrum

- CRDM flux at Earth can be expressed as

$$\frac{d\Phi_\chi}{dT_\chi} = D_{\rm eff}\,\frac{\rho_\chi}{m_\chi}\sum_i \int_{T_i^{\rm min}(T_\chi)}^{\infty} dT_i\,\frac{d\sigma_{\chi i}}{dT_\chi}\,\frac{d\Phi_i}{dT_i} \qquad \text{with} \qquad \frac{d\sigma_{\chi i}}{dT_\chi} = \frac{d\sigma_{\chi i}^{\rm el}}{dT_\chi} + \frac{d\sigma_{\chi i}^{\rm DIS}}{dT_\chi}$$

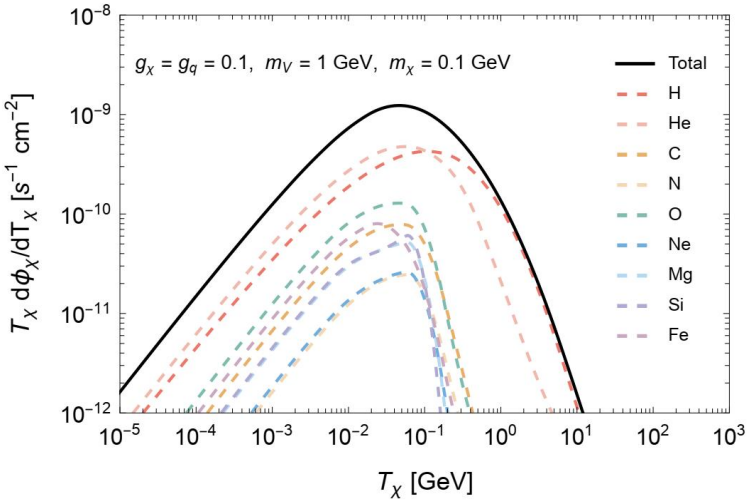

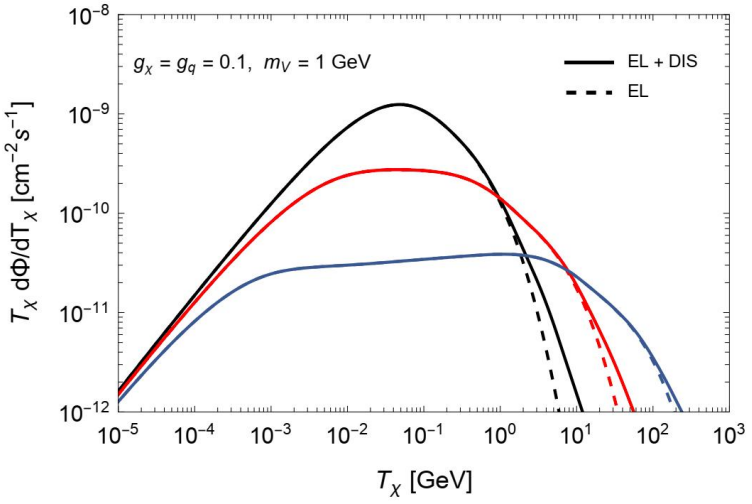

with DM mass is set as **100 MeV**, **10 MeV**, and **1 MeV**

CRDM track length spectrum

- The CRDM induced differential recoil rate of mineral nuclei is

$$\frac{d\Gamma_j}{dT_j} = \int_{T_\chi^{\min}(T_j)}^{\infty} dT_\chi \frac{d\sigma_{\chi j}}{dT_j} \frac{d\Phi_\chi}{dT_\chi}$$

  note that we care the low nuclear recoil energies $T_j \leq \mathcal{O}(0.1)\ GeV$, we restrict our analysis to elastic CRDM–nucleus scattering

- The differential rate of tracks with reconstructed length x_T for an exposure ϵ is given by

$$\frac{dR}{dx_T} = \epsilon \sum_j \frac{\xi_j}{m_j} \frac{d\Gamma_j}{dT_j} \frac{dT_j}{dx_T}$$

  where ξ_j denotes the mass fraction of element j, dT_j/dx_T is the stopping power, evaluated using SRIM, Ions with charge Z ≤ 2 do not produce persistent tracks

CRDM track length spectrum

- In this work, we adopt coarser resolution (e.g., ~ 15 nm) for larger samples (e.g.,~ 100 g)
- The expected number of events in the i-th bin, $x_T \in [x_a, x_b]$ is:

$$N_i(x_a, x_b) = \int_0^\infty dx_T \, W(x_T; x_a, x_b) \, \frac{dR}{dx_T}$$

with the window function $$W(x_T; x_a, x_b) = \frac{1}{2}\left[\mathrm{erf}\left(\frac{x_T - x_a}{\sqrt{2}\sigma_{x_T}}\right) - \mathrm{erf}\left(\frac{x_T - x_b}{\sqrt{2}\sigma_{x_T}}\right)\right]$$

- Two representative minerals are considered, Gypsum and Olivine
- Three background are considered, neutrinos, neutrons, and ^{234}Th

Signal and background spectra are computed using ***paleoSpec***

CRDM track length spectrum

- The binned track length spectrum in Gypsum for the vector-mediator model with $g_\chi = g_q = 0.7$ and $m_V = 1$ GeV

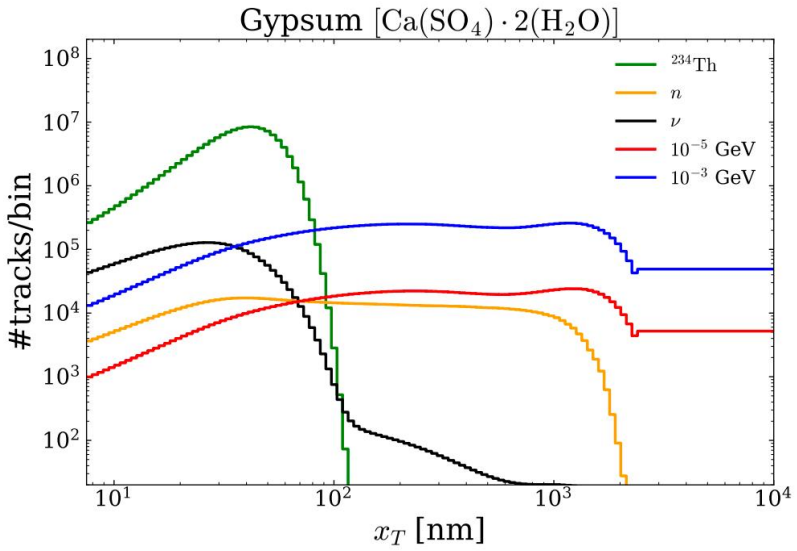

- We choose the upper edge of this bin at $x_T = 10$ μm and set its lower boundary such that the expected number of neutron-induced background events is below 0.5

- The projected sensitivities is derived by using the public code ***paleoSens***

Paleo detector constraints

- The expected number of CRDM events in XENONnT is:

$$N_{\mathrm{CRDM}} = \frac{\epsilon}{m_{\mathrm{Xe}}} \int_{T_{\mathrm{exp}}^{\mathrm{min}}}^{T_{\mathrm{exp}}^{\mathrm{max}}} dT_{\mathrm{Xe}} \frac{d\Gamma_{\mathrm{Xe}}}{dT_{\mathrm{Xe}}} \qquad \text{with} \qquad \epsilon = 3.1 \ \mathrm{t\,yr}$$

the 90% C.L.upper limit $N_{Xe}^{DM}(3.8\ keV \leq T_{Xe} \leq 64.1\ keV) < 35.87$

XENONnT

Olivine

Gypsum

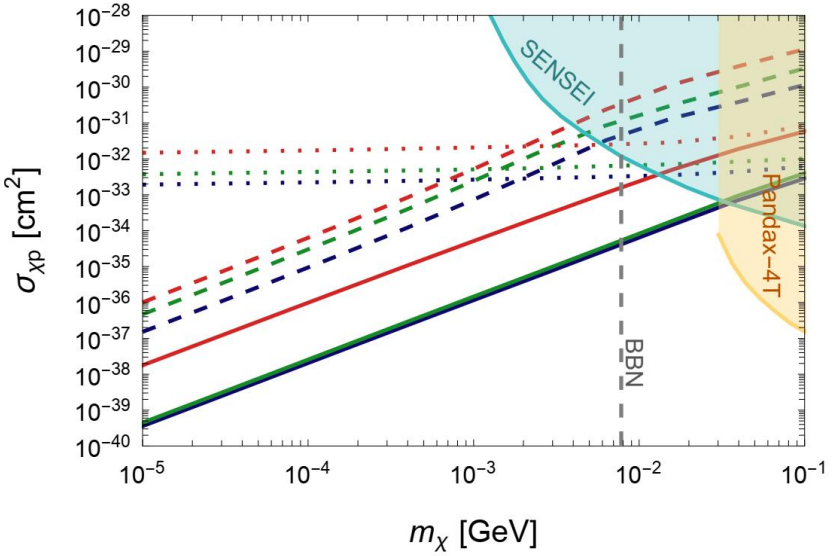

$\sigma_{\chi p}$

$m_V = 10\ MeV$

$m_V = 1\ GeV$

Summary

- The high-energy cosmic rays can accelerate DM and provide a new window for detecting light DM;
- Due to the large effective exposure, the paleo detector can be regarded as an efficient new method to explore the nature of DM;
- For two benchmark models, paleo-detectors yield stronger constraints on the DM–proton cross section than conventional direct detection.

Thank you